

Development of a Comprehensive Model for Diffusion-Controlled Free-Radical Copolymerization Reactions

A. Keramopoulos and C. Kiparissides*

Department of Chemical Engineering and Chemical Process Engineering Research Institute, Aristotle University of Thessaloniki, P.O. Box 472, Thessaloniki, Greece 540 06

Received June 11, 2001; Revised Manuscript Received December 10, 2001

ABSTRACT: In the present study a comprehensive mathematical model for diffusion-controlled free-radical copolymerization reactions is developed. Termination and propagation rate constants as well as initiator efficiency are expressed in terms of a reaction-limited term and a diffusion-limited one. The contribution of the latter term to the apparent rate constants is described in terms of the diffusion coefficients of the corresponding species (e.g., polymer chains, monomers, primary radicals), calculated using the generalized free-volume theory of Vrentas and Duda for a ternary system, and an effective reaction radius. The predictive capabilities of the present model are demonstrated by simulating three free-radical polymerization systems, namely, the bulk copolymerizations of styrene–methyl methacrylate, styrene–acrylonitrile, and *p*-methylstyrene–methyl methacrylate. It is shown that the model predictions are in excellent agreement with experimental data on monomer conversion, average molecular weights, and copolymer composition, reported in the open literature under various experimental conditions.

Introduction

The synthesis of linear and branched copolymers by free-radical reactions is of significant economic importance to the polymer industry, for the copolymerization of two or more monomers can lead to the production of polymers with desired physical, chemical, and mechanical end-use properties. Free-radical random copolymers are typically obtained as a mixture of macromolecules with different composition, chain length, degree of branching, and chain sequence characteristics. Controlling the copolymer chain microstructure and, thus, the end-use properties of the polymer requires a thorough understanding of the effects of polymerization kinetics and physical transport processes on the polymerization rate and molecular weight and compositional chain developments.

It is important to mention that, besides the conventional chemical kinetics, physical phenomena related to the diffusion of various chemical reactive species play a significant role in free-radical polymerizations. Reactions, which are influenced by diffusion phenomena, include termination of “live” macroradicals, growth of “live” polymer chains, and chemical initiation reactions. Diffusion-controlled termination, propagation, and initiation reactions have been related to the well-known phenomena of gel effect, glass effect, and cage effect, respectively. The gel effect, or Trommsdorff–Norrish effect, has been attributed to the decrease of the termination rate constant caused by a decrease of the mobility of polymer chains. This phenomenon strongly affects the final polymer molecular properties, since it leads to a broader molecular weight distribution. It can also cause the thermal runaway of a polymerization reactor. The glass effect has been related to the decrease of the propagation rate constant, caused by a decrease of the mobility of the monomer molecules. A consequence of this phenomenon is the “freezing” of the reaction mixture at conversions below 100%. At the

limiting conversion, the glass transition temperature of the polymer/monomer mixture becomes equal to the polymerization temperature. Chemical initiation involves the decomposition of initiator molecules to form very active primary radicals capable of initiating new polymer chains. However, because of the very close proximity of the generated radicals, not all of them can eventually escape from their “cages” to react with monomer molecules. In fact, some primary radicals will either self-terminate or react with other nearest-neighbor molecules before diffusing out of their “cages”. Reported experimental results^{1,2} show that initiator efficiency can dramatically change with monomer conversion. This indicates that diffusion of primary radicals can be influenced by the physical and transport properties of the reaction medium.

In the past 30 years, a great number of mathematical models, dealing with the quantitative description of diffusion-controlled phenomena in free-radical homopolymerizations, have been published in the open literature.^{3–16} However, the number of publications on diffusion-controlled free-radical copolymerizations is very limited. Garcia-Rubio et al.¹⁷ developed a mathematical model to describe the kinetics of styrene–acrylonitrile bulk copolymerization. The original free-volume model of Marten and Hamielec⁴ was properly revised to account for diffusion-controlled termination and propagation reactions in free-radical copolymerizations. Conversion, copolymer composition and monomer chain sequence predictions were in good agreement with the experimental data. Following this work, several kinetic models, based on Marten and Hamielec’s free-volume homopolymerization model, were published on different copolymerization systems.^{18–20} In general, model predictions were in reasonable agreement with experimental data. However, a significant discrepancy between predicted and experimental weight-average molecular weights was observed in all studies.

Hwang et al.²¹ presented a mathematical model for the styrene–acrylonitrile bulk copolymerization. The free-volume theory⁴ was employed to describe the

* Corresponding author. Tel + 30310 99 6211; fax +310 99 6198; e-mail cypress@alexandros.cperi.certh.gr.

dependence of propagation and termination rate constants on monomer conversion. The pseudo-kinetic rate constant method was applied to reduce the complexity of the copolymerization rate expressions. Model predictions on monomer conversion and copolymer composition were found to be in good agreement with the respective experimental measurements. However, no comparison of model predictions with available experimental data on molecular weight averages was reported. Finally, Sharma et al.²² extended their original homopolymerization model⁷ to copolymerization systems. Their theoretical diffusion-controlled model, based on an extension of the Fujita–Doolittle free-volume theory, accounted for both the gel and glass effects. A simple copolymerization kinetic mechanism was employed to describe the kinetics of styrene–methyl methacrylate copolymerization. However, only a single experimental run (e.g., on monomer conversion) was employed for comparison with model predictions.

In the present work, a generalized mathematical framework is developed to describe diffusion-controlled reactions in free-radical copolymerizations. The initiator efficiency as well as the propagation and termination rate constants is expressed in terms of a reaction-limited term and a diffusion-limited one. The generalized free-volume theory of Vrentas and Duda for ternary systems^{23–25} is utilized to estimate the self-diffusion coefficients of the pertinent reactive species. The ability of the new mathematical model to describe diffusion-controlled reactions in free-radical copolymerizations is demonstrated by its application to several systems, including the styrene–acrylonitrile, styrene–methyl methacrylate, and *p*-methylstyrene–methyl methacrylate. To our knowledge, this is the first attempt to predict the variation of conversion, average molecular weights, and copolymer composition in free-radical copolymerization reactions by taking into account simultaneously the free-volume dependence of termination and propagation rate constants as well as of initiator efficiency on the polymerization conditions.

Calculation of the Monomer and Polymer Diffusion Coefficients

The diffusion of the various reactive species has to be adequately described in a kinetic copolymerization model by taking into account the continuous change of the transport properties of the reaction medium during polymerization. The generalized free-volume theory of Vrentas and Duda^{23,26,27} is generally accepted as one of the most successful approaches for calculating the molecular diffusion coefficients of the various reactive species in a polymerization medium.

Thus, following the original developments of Vrentas and Duda²³ for a ternary system, one can define four independent diffusion coefficients (e.g., D_{11} , D_{12} , D_{21} , and D_{22}) to describe fully the molecular fluxes of the two monomers in a copolymerization system (e.g., two monomers and polymer). It should be pointed out that the free-volume theory, like most fundamental theories of diffusion, results in expressions that describe the self-diffusion coefficient of a species in solution. However, Vrentas et al.²⁵ showed that for the case of a ternary system comprising two low molecular weight species and a polymer, at relatively low concentrations of the penetrant monomers, the principal diffusion coefficients (D_{11} , D_{22}) are significantly larger than the cross-diffu-

sion coefficients (D_{12} , D_{21}) and approximately equal to the self-diffusion coefficients (D_{m1} , D_{m2}) of the two monomers.

Considering the distribution of the available hole free volume among all the jumping units of monomer 1, monomer 2, and copolymer, the resulting expressions for the monomer diffusion coefficients, D_{m1} and D_{m2} , will be given by²³

$$D_{m1} = D_{01} \exp[-\gamma_m(\omega_1 V_1^* + \omega_2 V_2^* \xi_{1p}/\xi_{2p} + \omega_p V_p^* \xi_{1p})/V_{FH}] \quad (1)$$

$$D_{m2} = D_{02} \exp[-\gamma_m(\omega_1 V_1^* \xi_{2p}/\xi_{1p} + \omega_2 V_2^* + \omega_p V_p^* \xi_{2p})/V_{FH}] \quad (2)$$

where the subscripts 1, 2, and p refer to the two monomers and the copolymer, respectively. γ_m is an overlap factor.²³ D_{0i} , ω_i , and V_i^* denote the respective preexponential constant of the diffusion coefficient, the weight fraction, and the specific critical hole free volume of species “*i*” in the mixture. Note that the value of V_i^* can be estimated by the group contribution method of Haward,²⁸ based on the chemical composition of the species of interest.

The parameter ξ_{ip} is defined as the ratio of the critical molar volume of the jumping unit of species “*i*” to that of the jumping unit of the polymer, V_{pj} :

$$\xi_{ip} = V_i^* MW_j / V_{pj} \quad (3)$$

Because of the inherent difficulty in determining the molecular weight of the polymer jumping unit, an empirical expression has been proposed³⁰ for its calculation in terms of the glass transition temperature of the copolymer:

$$V_{pj} = [0.6224 T_{gp} - 86.95], \quad T_{gp} \geq 295 \text{ K} \quad (4)$$

$$V_{pj} = [0.0925 T_{gp} + 69.47], \quad T_{gp} \leq 295 \text{ K} \quad (5)$$

Finally, V_{FH} is the average free volume of the mixture given by the weighted sum of the free volumes of the three components in the reaction mixture:^{10,23}

$$V_{FH} = [\alpha_{p0} + \alpha_p(T - T_{gp})] V_p^* \omega_p + [\alpha_{m10} + \alpha_{m1}(T - T_{gm1})] V_1^* \omega_1 + [\alpha_{m20} + \alpha_{m2}(T - T_{gm2})] V_2^* \omega_2 \quad (6)$$

where α_i and α_{i0} are the difference in the thermal expansion coefficient above and below the glass transition temperature and the fractional free volume at the glass transition temperature, respectively.

The copolymer glass transition temperature, T_{gp} , depends on the copolymer composition, F_{ni} , and the glass transition temperatures of the respective homopolymers (T_{gp1} and T_{gp2}). T_{gp} can be calculated from the Suzuki et al.³⁰ relationship:

$$T_{gp} = F_{n1} T_{gp1} + F_{n2} T_{gp2} + (R_T/100)(T_{gp12} - \bar{T}_{gp}) \quad (7)$$

where \bar{T}_{gp} is the mean glass transition temperature of the two homopolymers:

$$\bar{T}_{gp} = (T_{gp1} + T_{gp2})/2 \quad (8)$$

T_{gp12} is the glass transition temperature of the corresponding strictly alternating copolymer,³⁰ and R_T , the so-called “run number”, is defined as the average

number of both 1 and 2 monomer chain sequences occurring in a copolymer per 100 monomer units. R_T can be estimated from the following relation:³⁰

$$R_T = 400F_{n1}F_{n2}/[1 + (1 + 4F_{n1}F_{n2}(r_1r_2 - 1))^{1/2}] \quad (9)$$

where r_1r_2 is the product of the monomer reactivity ratios.

Following the original developments of Achilias and Kiparissides,¹² the translational diffusion coefficient of the polymer chains will be given by

$$D_p = (D_{p0}/M_w^2) \exp[-\gamma_p(\omega_1 V_1^*/\xi_{1p} + \omega_2 V_2^*/\xi_{2p} + \omega_p V_p^*/V_{FH})] \quad (10)$$

where M_w is the weight-average molecular weight of the copolymer. D_{p0} is a preexponential factor calculated at zero polymer concentration by solving eq 10 for D_{p0} and estimating D_p using the Stokes–Einstein diffusion equation:¹²

$$D_p = k_B T / (6\pi\eta_{\text{mix}}R_H) \quad (11)$$

where k_B is the Boltzmann constant and η_{mix} is the solution viscosity of the two monomers calculated using the one-constant method of Grunberg and Nissan:³¹

$$\ln \eta_{\text{mix}} = x_1 \ln \eta_1 + x_2 \ln \eta_2 + x_1 x_2 G_{12} \quad (12)$$

where x_i and η_i are the mole fraction and viscosity of monomer “ i ”, respectively. G_{12} is a binary interaction parameter for the two monomers and is calculated using a group contribution method.³¹ The polymer hydrodynamic radius, R_H , will depend on the intrinsic viscosity of the copolymer solution and the weight-average molecular weight of the copolymer and is calculated from the Einstein equation at infinite dilution:³²

$$R_H = \left(\frac{3}{10\pi N_A} [\eta] M_w \right)^{1/3} \quad (13)$$

To account for the segmental diffusion of the growing polymer chains, the translational diffusion coefficient, D_p , is multiplied by the factor F_{seg} .¹²

$$D_{pe} = F_{\text{seg}} D_p \quad (14)$$

where D_{pe} is the effective diffusion coefficient of the polymer chains. F_{seg} accounts for the probability of two “live” polymer chains to react when their active centers come into close proximity and is given by^{12,33}

$$F_{\text{seg}} = r_e^3 [\pi r_e + 6(\sqrt{2})\alpha_{\text{seg}} r_B] / (16\pi r_B^4) \quad (15)$$

r_e and r_B denote the Kuhn’s segment length and the distance of the chain end from the growing radical sphere center,³³ respectively. α_{seg} is a parameter depending on the initiator type and the composition of the mixture.

It should be noted that, in deriving the above equations, we have assumed that the mass fraction of the initiator is very small compared to the mass fractions of the monomers and copolymer.

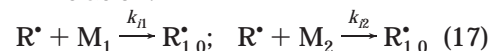
Diffusion-Controlled Initiation Reaction

In the presence of a thermally decomposed initiator, copolymer chain initiation proceeds according to the

following kinetic mechanism:



polymer chain initiation:



Following the original work of Achilias and Kiparissides,¹² it is assumed that primary radicals, R^* , are generated within an initiator reaction sphere of radius r_{11} , placed inside a larger diffusion sphere of radius r_{12} . Let us further assume that only radicals escaping from the larger diffusion sphere can react with the monomers to initiate new copolymer chains. Let $[R^*]'$ be the effective concentration of primary radicals outside the diffusion sphere, r_{12} . Assuming a one-dimensional steady-state mass-transfer process, the diffusion rate of primary radicals out of the “cage” of radius r_{12} will be equal to the extensive chain initiation reaction rate between the monomers and the escaping primary radicals, R_1' :

$$-4\pi r^2 D_1 \frac{d[R^*]'}{dr} = R_1' \quad (18)$$

where D_1 is the diffusion coefficient of the primary radicals, given by the following equation:¹²

$$D_1 = D_{10} \exp[-\gamma_1(\omega_1 V_1^*/\xi_{1p} + \omega_2 V_2^*/\xi_{2p} + \omega_p V_p^*/V_{FH})] \quad (19)$$

Equation 18 will satisfy the following boundary conditions:

$$[R^*] = [R^*]' \text{ at } r = r_{11}; \quad [R^*] = [R^*]' \text{ at } r = r_{12} \quad (20)$$

Assuming that $r_{12} \gg r_{11}$ and integrating eq 18, we obtain

$$4\pi r_{11} D_1 ([R^*] - [R^*]') = R_1' \quad (21)$$

The extensive chain initiation reaction rate, R_1' , will be given by

$$R_1' = (k_{i10}[R^*]'[M_1] + k_{i20}[R^*]'[M_2]) V_1 \quad (22)$$

where V_1 denotes an effective chain initiation reaction volume which is assumed to be equal to $4\pi r_{12}^3/3$. Thus, from eqs 21 and 22, one can estimate the effective primary radical concentration:

$$[R^*]/[R^*]' = 1 + [(k_{i10}[M_1] + k_{i20}[M_2])r_{12}^3]/3r_{11}D_1 \quad (23)$$

Assuming that the quasi-steady-state approximation for primary radicals holds true, one can express the intensive chain initiation reaction rate, R_1 , as follows:

$$R_1 = (k_{i10}[M_1] + k_{i20}[M_2])[R^*]' = 2fk_d[I] \quad (24)$$

where f is the initiator efficiency. At very low monomer conversions, the diffusion rate of primary radicals out of the “cage” will be very fast; thus, one can assume that $[R^*] \cong [R^*]'$. Therefore,

$$R_1 = (k_{i10}[M_1] + k_{i20}[M_2])[R^*] = 2f_0k_d[I] \quad (25)$$

where f_0 denotes the initiator efficiency at zero monomer conversion. Dividing eq 25 by eq 24 and substituting

eq 23 into the resulting expression, we obtain

$$f^{-1} = f_0^{-1} + (k_{i10}[M_1] + k_{i20}[M_2])r_{i2}^3 / (3r_{i1}f_0D_i) = f_0^{-1}(1 + f_D^{-1}) \quad (26)$$

From eqs 19 and 26, one can easily conclude that the overall initiator efficiency, f , will depend on the monomer concentrations $[M_1]$ and $[M_2]$, as well as on D_i , which in turn depends on the free volume of the reaction mixture. Thus, at very low monomer conversions the contribution of the diffusion-controlled term, f_D^{-1} , in eq 26 will be insignificant, and thus, $f \cong f_0$. On the other hand, at high monomer conversions (e.g., high solution viscosities and low values of the available free volume), the contribution of the f_D^{-1} term in eq 26 will be significant (e.g., $f_D^{-1} \gg 1$), and thus, $f \approx f_0 f_D^{-1}$. In the latter case, the overall initiator efficiency will decrease with the extent of the copolymerization reaction.

Diffusion-Controlled Termination Reactions

Following the original work of Achilias and Kiparissides,¹² the termination rate constants (k_{t11} and k_{t22}) can be expressed as follows:

$$k_{tii} = k_{tii}^d + k_{tii}^{\text{res}} \quad (27)$$

where the subscript “ i ” refers to the terminal unit of the macroradical. k_{tii}^d and k_{tii}^{res} denote the diffusion-controlled termination rate constant between two “live” polymer chains of the same type (e.g., having the same terminal unit) and the so-called “residual termination” rate constant, respectively.

Accordingly, k_{tii}^d is subsequently expressed in terms of the intrinsic termination rate constant, k_{t0ib} , and a diffusion-controlled term:

$$\frac{1}{k_{tii}^d} = \frac{1}{k_{t0ib}} + \frac{1}{4\pi r_{ti} D_{pe} N_A} \quad (28)$$

Notice that the contribution of the diffusion-controlled term in eq 28 has been written according to the recent work of Litvinenko and Kaminsky.³⁴ r_{ti} is an effective termination radius for the “live” polymer chains:¹²

$$r_{ti} = \{\ln[1000\tau_i^3 / (N_A \lambda_{00}^i \pi^{3/2})]\}^{1/2} / \tau_i \quad (29)$$

$$\tau_i = [3 / (2j_{ci} \delta_i^2)]^{1/2} \quad (30)$$

δ_i , λ_{00}^i , and j_{ci} are the average root-mean-square end-to-end distance of a polymer chain, the total concentration of the “live” polymer chains of type “ i ”, and the entanglement spacing between polymer chains, respectively. j_{ci} can be calculated by¹²

$$j_{ci}^{-1} = j_{c0i}^{-1} + 2\phi_p / X_{c0i} \quad (31)$$

X_{c0i} and j_{c0i} are the critical degree of polymerization for the entanglement of polymer chains of type “ i ” and the critical value of j_{ci} at zero conversion, respectively.

At very high conversions, the self-diffusion coefficient becomes very small, resulting in an unrealistically low value of k_{tii} . The reason is that eq 10 does not account for the mobility of the growing polymer chains caused by the monomer propagation reactions. This phenom-

enon is known as residual termination, and its rate constant can be expressed as¹²

$$k_{tii}^{\text{res}} = A_{pi} k_{pji} [M_j] \quad (32)$$

where the proportionality rate constant, A_{pi} , can be estimated from the volume-swept-out model:³⁵

$$A_{pi} = \pi \delta_i^3 j_{ci} N_A \quad (33)$$

In the present study, the cross termination rate constants (e.g., $k_{t12} = k_{t21}$) were calculated using the following correlation:

$$\phi_t = k_{t12} / [2(k_{t11} k_{t22})^{1/2}] \quad (34)$$

Diffusion-Controlled Propagation Reactions

At very high conversions, even the movement of small molecules is hindered. As a result, the propagation reactions become diffusion-controlled as well. In the present work, the propagation rate constants (k_{p11} and k_{p22}) were expressed as in the original paper of Achilias and Kiparissides,¹² taking into account the correction proposed by Litvinenko and Kaminsky.³⁴

$$\frac{1}{k_{pii}} = \frac{1}{k_{p0ii}} + \frac{1}{4\pi r_{mi} D_{mi} N_A} \quad (35)$$

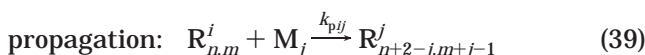
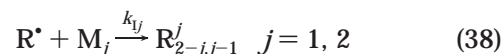
The effective reaction radius r_{mi} was assumed to be equal to the termination reaction radius, r_{ti} , while the monomer diffusion coefficients were calculated from eqs 1 and 2.

The cross-propagation rate constants (k_{p12} and k_{p21}) were estimated in terms of the respective reactivity ratios r_1 and r_2 and the values of k_{p11} and k_{p22} :

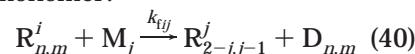
$$r_1 = k_{p11} / k_{p12}, \quad r_2 = k_{p22} / k_{p21} \quad (36)$$

Kinetic Model Developments

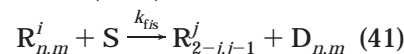
A comprehensive kinetic mechanism was employed to describe all the elementary reactions occurring in a chemically initiated free-radical copolymerization. Thus, besides the conventional reactions (e.g., initiation, propagation, and termination), the copolymerization mechanism included chain transfer to monomer, to polymer, and to chain transfer agent as well as a terminal double-bond polymerization reaction. In particular, the following elementary reactions were considered.^{36,37}



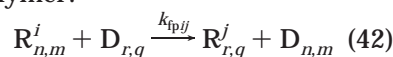
chain transfer to monomer:



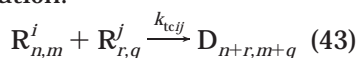
chain transfer to modifier (CTA):



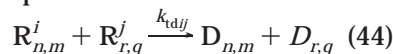
chain transfer to polymer:



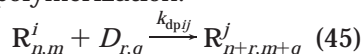
termination by combination:



termination by disproportionation:



terminal double bond polymerization:



In the above kinetic scheme, the symbols I, R^{*}, M_j (j = 1, 2), and S denote the initiator, primary radicals, monomer, and chain transfer agent (e.g., modifier) molecules, respectively. The present copolymerization mechanism comprises two chain initiation reactions, four propagation, four chain transfer to monomer, two chain transfer to modifier, four chain transfer to polymer, three termination by combination, three termination by disproportionation, and four terminal double bond reactions. That is a total of 26 elementary reactions. It was assumed that no depropagation reactions occurred and penultimate monomer effects were negligible.

The symbols R_{n,m}ⁱ and D_{n,m} identify the respective "live" and "dead" copolymer chains. The subscripts *n* and *m* denote the respective degrees of polymerization for monomer 1 (M₁) and monomer 2 (M₂). Finally, the superscript "i" refers to the ultimate monomer unit in the radical chain, which can be either of type M₁ or M₂.

Copolymerization Rate Functions. The respective net rates of production of "live" and "dead" copolymer chains can be obtained by combining the reaction rates of the relevant elementary reactions, describing the generation and consumption of "live" and "dead" polymer chains. On the basis of the above kinetic mechanism of free-radical copolymerization, the following general rate functions can be derived:³⁶

"live" copolymer chains of type "i" of total length, *n* + *m*:

$$r_{R_{n,m}^i} = (k_{I^*} P R^* M_i + \sum_{j=1}^2 k_{tj} M_i R_{0,0}^j + k_{fis} S R_{0,0}^i) \delta(n + m - 2, m + 1 - i) + \sum_{j=1}^2 k_{pj} M_i R_{n+i-2, m+1-i}^j - \sum_{j=1}^2 k_{pji} M_j R_{n,m}^i - A_i R_{n,m}^i + \sum_{j=1}^2 k_{fpj} R_{0,0}^j n^{i-1} m^{i-1} D_{n,m} - \sum_{j=1}^2 k_{dpj} R_{n,m}^i \sum_{r=0}^{\infty} \sum_{q=0}^{\infty} D_{r,q} + \sum_{j=1}^2 k_{dpj} \sum_{r=0}^{\infty} \sum_{q=0}^{\infty} D_{r,q} R_{n-r, m-q}^j \quad (46)$$

"dead" copolymer chains of total length, *n* + *m*:

$$r_{D_{n,m}} = \sum_{j=1}^2 (A_j - \sum_{f=1}^2 k_{tcjf} R_{0,0}^f) R_{n,m}^i - \sum_{i=1}^2 \sum_{j=1}^2 k_{fpj} R_{0,0}^i n^{i-1} m^{j-1} D_{n,m} + \frac{1}{2} \sum_{f=1}^2 \sum_{j=1}^2 k_{tcij} \sum_{r=1}^2 \sum_{q=1}^2 k_{tcij} \sum_{r=1}^{n-1} \sum_{q=1}^{m-1} R_{r,q}^i R_{n-r, m-q}^j - \sum_{i=1}^2 \sum_{j=1}^2 k_{dpj} R_{0,0}^i D_{n,m} \quad (47)$$

where

$$A_i = \sum_{j=1}^2 (k_{fij} M_j + k_{tj} R_{0,0}^j) + k_{fis} S + \sum_{j=1}^2 k_{fpj} \sum_{r=0}^{\infty} \sum_{q=0}^{\infty} r^{i-1} q^{j-1} D_{r,q} \quad (48)$$

R_{0,0}ⁱ denotes the total concentration of "live" polymer chains of type "i" and is given by

$$R_{0,0}^i = \sum_{n=0}^{\infty} \sum_{m=0}^{\infty} R_{n,m}^i \quad (49)$$

δ(*n, m*) is the Kronecker's delta, given by

$$\delta(n, m) = \delta(n) \delta(m); \quad \delta(j) \equiv \begin{cases} 1 & \text{for } i = 0 \\ 0 & \text{for } i \neq 0 \end{cases} \quad (50)$$

Application of the fundamental mass conservation equation to the various molecular species of interest (e.g., "live" and "dead" polymer chains, etc.) typically results in an infinite system of differential equations.³⁶ To reduce the high dimensionality of the numerical problem, several mathematical techniques have been proposed in the literature.³⁸ In the present study, the method of moments was utilized to recast the "infinite" system of dynamic molar balance equations into a low-order system of differential moment equations that can be easily solved.

The method of moments is based on the statistical representation of the average molecular properties of the polymer in terms of the leading moments of the number chain length distributions of the "live" and "dead" polymer chains. For a copolymerization system one needs to introduce bivariate distributions with respect to the degrees of polymerization of monomers M₁ and M₂ to describe the molecular and compositional chain developments. In particular, the bivariate chain length-copolymer composition (CLCC) distributions associated with the "live" and "dead" copolymer chains were employed. Accordingly, the respective moments for "live" and "dead" copolymer chains were defined as

$$\lambda_{k,l}^i = \sum_{n=1}^{\infty} \sum_{m=1}^{\infty} n^k m^l R_{n,m}^i; \quad k, l = 0, 1, 2 \text{ and } i = 1, 2 \quad (51)$$

$$\mu_{k,l} = \sum_{n=1}^{\infty} \sum_{m=1}^{\infty} n^k m^l D_{n,m}; \quad k, l = 0, 1, 2 \quad (52)$$

The relevant rate functions for the moments λ_{k,l}ⁱ and μ_{k,l} can be obtained from eqs 46 and 47 by multiplying each term by n^km^l and summing the resulting expressions over the total variations of *n* and *m*. The final

equations for the corresponding moment rate functions are³⁶

$$r_{\lambda_{k,l}^i} = (k_{Ii}PRM_i + \sum_{j=1}^2 k_{fij}M_j\lambda_{00}^j + k_{fis}S\lambda_{00}^i)\delta(I) + \sum_{j=1}^2 k_{pji}M_j \left[(2-i) \sum_r^k \binom{k}{r} \lambda_{r,l}^j + (i-1) \sum_r^l \binom{l}{r} \lambda_{k,r}^j \right] - \sum_{j=1}^2 k_{pji}M_j \lambda_{k,l}^i - (A_i' + \sum_{j=1}^2 k_{tcij}\lambda_{00}^j) \lambda_{k,l}^i + \sum_{j=1}^2 k_{fpj}\lambda_{00}^j \mu_{k+2-j,1+i-1} - \sum_{j=1}^2 k_{dpj}\lambda_{k,l}^i \mu_{00} + \sum_{j=1}^2 k_{dpji} \sum_p^k \sum_q^l \binom{k}{p} \binom{l}{q} \mu_{pq} \lambda_{k-p,l-q}^j \quad (53)$$

$$r_{\mu_{k,l}} = \sum_{j=1}^2 A_j' \lambda_{k,l}^j + \frac{1}{2} \sum_{r=1}^2 \sum_{q=1}^2 k_{tcrq} \sum_i^k \sum_j^l \binom{k}{i} \binom{l}{j} \lambda_{i,j}^r \lambda_{k-i,l-j}^q - \sum_{i=1}^2 \sum_{j=1}^2 k_{fpij}\lambda_{00}^j \mu_{k+2-j,1+j-1} - \sum_{i=1}^2 \sum_{j=1}^2 k_{dpij}\lambda_{00}^j \mu_{k,l} \quad (54)$$

where

$$A_i' = \sum_{j=1}^2 k_{fij}M_j + k_{fis}S + \sum_{j=1}^2 k_{tdij}\lambda_{00}^j + \sum_{j=1}^2 k_{fpij}\mu_{2-j,j-1} \quad (55)$$

Reactor Design Equations. Based on the above definitions of the moment rate functions, the basic design equations for a batch copolymerization reactor can be easily derived.

$$\text{initiator: } \frac{d(VI)}{dt} = -Vk_d I \quad (56)$$

monomers:

$$\frac{d(VM_1)}{dt} = Vr_{M1} = -V\{[(k_{p11} + k_{f11})\lambda_{00}^1 + (k_{p21} + k_{f21})\lambda_{00}^2]M_1 + k_{I1}PRM_1\} \quad (57)$$

$$\frac{d(VM_2)}{dt} = Vr_{M2} = -V\{[(k_{p12} + k_{f12})\lambda_{00}^1 + (k_{p22} + k_{f22})\lambda_{00}^2]M_2 + k_{I2}PRM_2\} \quad (58)$$

modifier (chain transfer agent):

$$\frac{d(VS)}{dt} = -V\{[(k_{f1s})\lambda_{00}^1 + k_{f2s}\lambda_{00}^2]S\} \quad (59)$$

volume contraction:

$$\frac{dV}{dt} = -V\left[r_{M1}(MW_1)\left(\frac{1}{d_1} - \frac{1}{d_p}\right) + r_{M2}(MW_2)\left(\frac{1}{d_2} - \frac{1}{d_p}\right)\right] \quad (60)$$

chain length distribution moments:

$$\frac{d(V\lambda_{k,l}^i)}{dt} = Vr_{\lambda_{k,l}^i}; \quad i = 1, 2 \quad (61)$$

$$\frac{d(V\mu_{k,l})}{dt} = Vr_{\mu_{k,l}} \quad (62)$$

fractional monomer conversion:

$$X = \frac{V_0(M_{10} + M_{20}) - V(M_1 + M_2)}{V_0(M_{10} + M_{20})} \quad (63)$$

On the basis of the double moments of the “dead” CLCC distribution, one can easily calculate the cumulative number- and weight-average copolymer compositions, (e.g., F_{n1} and F_{w1}):

$$F_{n1} = \mu_{1,0}/(\mu_{1,0} + \mu_{0,1}) \quad (64)$$

$$F_{w1} = (MW_1\mu_{2,0} + MW_2\mu_{1,1})/(MW_1\mu_{2,0} + (MW_1 + MW_2)\mu_{1,1} + MW_2\mu_{0,2}) \quad (65)$$

as well as the cumulative number- and weight-average molecular weights of the copolymer:

$$M_n = [(\mu_{1,0} + \mu_{0,1})/\mu_{0,0}](F_{n1}MW_1 + F_{n2}MW_2) \quad (66)$$

$$M_w = [(MW_1\mu_{2,0} + (MW_1 + MW_2)\mu_{1,1} + MW_2\mu_{0,2})/(MW_1\mu_{1,0} + MW_2\mu_{0,1})](F_{n1}MW_1 + F_{n2}MW_2) \quad (67)$$

where MW_1 and MW_2 are the molecular weights of monomers 1 and 2, respectively.

Results and Discussion

The predictive capabilities of the developed comprehensive model were demonstrated by its application to three copolymerization systems (e.g., styrene–acrylonitrile, styrene–methyl methacrylate, and *p*-methylstyrene–methyl methacrylate). In what follows, model predictions are compared with experimental measurements on monomer conversion, copolymer composition, and number- and weight-average molecular weights for the three selected copolymerization systems.

Bulk Copolymerization of Styrene–Acrylonitrile. The bulk copolymerization of styrene–acrylonitrile (SAN) proceeds in a single homogeneous phase when the initial styrene mole fraction is equal to or greater than 50%.³⁹ The copolymerization is readily initiated by azo or peroxy compounds.

To model the molecular and compositional chain developments in the SAN copolymerization, a comprehensive kinetic mechanism was considered. Both termination reactions were included (i.e., by disproportionation and combination) although the latter type of radical termination was considered to be the dominant one.³⁹ The formation of terminal double bonds (e.g., via chain transfer to monomer) and their subsequent reaction with “live” polymer chains (e.g., terminal double bond polymerization) were also included in the kinetic mechanism. On the other hand, transfer to polymer reactions were assumed to be negligible. Model predictions were compared with the experimental measurements of Garcia-Rubio³⁹ on monomer conversion, residual monomer mole fraction, and average molecular weights obtained for five different initial monomer compositions. In Table 1 the numerical values of all kinetic rate constants employed in the simulation of the

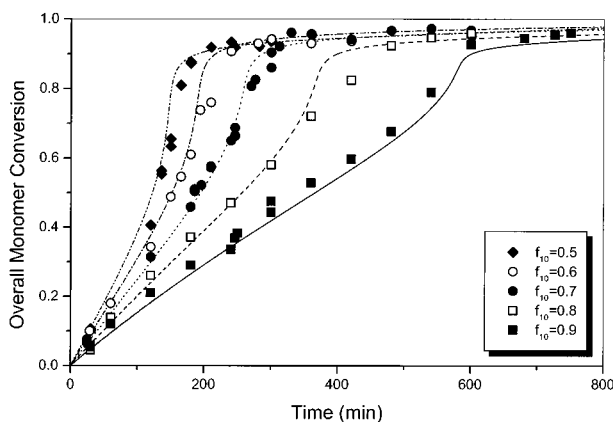


Figure 1. Predicted and experimental conversion–time histories for styrene–acrylonitrile copolymerization (polymerization temperature 60 °C, $[I_0] = 0.05$ M AIBN, experimental data from ref 39).

Table 1. Kinetic Rate Constants for the SAN Copolymerization

$k_{p11} = 6.54 \times 10^8 \exp(-7051/RT)$ (L/mol min) (ref 12)
$k_{p22} = 6.282 \times 10^9 \exp(-3663/RT)$ (L/mol min) (ref 20)
$r_1 = 0.36; r_2 = 0.078$ (ref 17)
$k_{tc11} = 7.53 \times 10^{10} \exp(-1677/RT)$ (L/mol min) (ref 43)
$k_{tc22} = 1.98 \times 10^{14} \exp(-5400/RT)$ (L/mol min) (ref 43)
$k_{td11} = 0; k_{td22} = 0$
$\phi_t = 16[(1 - f_{10}) \times 0.0625 + r_1 f_{10}]/[(1 - f_{10}) + r_1 f_{10}]$ (ref 44)
$k_{f11} = 1.38 \times 10^8 \exp(-12670/RT)$ (L/mol min) (ref 43)
$k_{f12} = 4.15 \times 10^9 \exp(-12670/RT)$ (L/mol min) (ref 43)
$k_{f22} = 2.77 \times 10^6 \exp(-5837/RT)$ (L/mol min)
$k_{f21} = 1.38 \times 10^7 \exp(-5837/RT)$ (L/mol min)
$k_{dp11} = 0.02 \times k_{p11}; k_{dp12} = k_{dp11}/r_1$
$k_{dp22} = 0.50 \times k_{p22}; k_{dp21} = k_{dp22}/r_2$
$k_d = 6.32 \times 10^{16} \exp(-30660/RT)$ (1/min) (ref 12)

Table 2. Physical and Transport Properties for the SAN Copolymerization System

$d_{m1} = 0.9236 - 0.887 \times 10^{-3}(T - 273.15)$ (g/cm ³) (ref 12)
$d_{m2} = 0.806 - 1.052 \times 10^{-3}(T - 293.15)$ (g/cm ³) (ref 20)
$d_{p1} = 1.085 - 6.05 \times 10^{-4}(T - 273.15)$ (g/cm ³) (ref 45)
$d_{p2} = 1.150$ (g/cm ³) (ref 46)
$MW_1 = 104.14; MW_2 = 53.06; M_{fl} = 68.1; f_0 = 0.58$ (ref 12)
$\delta_1 = \delta_2 = 7.4$ Å (ref 12)
$X_{c01} = 385; X_{c02} = 100$ (ref 12)
$\epsilon_{110}/D_{10} = 50.0; \epsilon_{120}/D_{10} = 30.0$ (s/cm ²) (calcd)
$\alpha_p = 2.5 \times 10^{-4}$ (ref 17); $\alpha_{m1} = 6.2 \times 10^{-4}$ (ref 6); $\alpha_{m2} = 1.25 \times 10^{-3}$ (K ⁻¹) (ref 17)
$\alpha_{p0} = 0.025; \alpha_{m10} = 0.040; \alpha_{m20} = 0.025$ (ref 6)
$T_{gm1} = 185.0$ K; $T_{gm2} = 190.38$ K (ref 17)
$V_{m1}^* = 0.912; V_{m2}^* = 1.135; V_{p1}^* = 0.835; V_{p2}^* = 0.949;$ $V_1^* = 0.912; (\text{cm}^3/\text{g})$ (calcd)
$r_{e1} = 16.9; r_{e2} = 16.5$ Å; $r_e = F_{n1}r_{e1}(1 - F_{n1})r_{e2}$ (Kuhn's segment length) (ref 47)
$\gamma_m = 0.33; \gamma_1 = 0.80; \gamma_p = 0.17; \alpha_{seg} = 0.2$
$D_{m10} = 1.97 \times 10^{-8}$ (cm ² /s) (ref 12); $D_{m20} = 5.0 \times 10^{-8}$ (cm ² /s)
$\log(\eta_1) = 528.64 \times (1/T - 1/276.71)$ cP (ref 12)
$\log(\eta_2) = 343.3 \times (1/T - 1/210.4)$ cP; $G_{12} = 0.333$
$[\eta] = 3.6 \times 10^{-5} M_w^{0.62}$ (l/g) (ref 46)

SAN copolymerization system are reported. In Table 2 the values of the physical and transport properties used in the calculation of diffusion-controlled rate constants are presented.

In Figure 1, conversion–time histories are plotted for five different values of the initial styrene mole fraction, f_{10} . Continuous and broken lines represent model predictions while discrete points denote the experimental conversion measurements. It is apparent that an excellent agreement exists between model predictions and experimental results. It is also evident that as the initial mole fraction of styrene decreases the polymerization

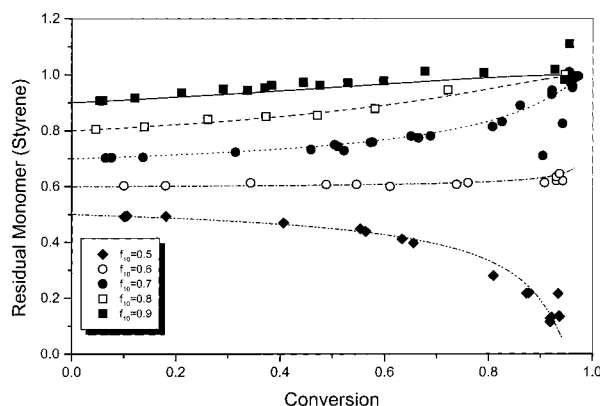


Figure 2. Residual mole fraction of styrene with respect to the overall monomer conversion (conditions same as in Figure 1).

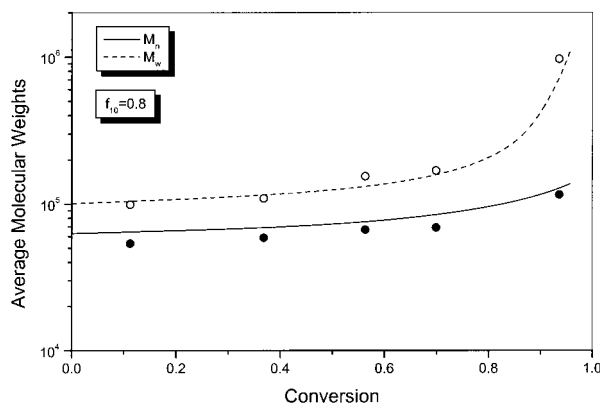


Figure 3. Weight- and number-average molecular weights with respect to the overall monomer conversion (conditions same as Figure 1).

rate increases due to the higher value of the acrylonitrile propagation rate constant. In Figure 2, the residual monomer mole fraction of styrene is plotted with respect to conversion for all five cases of f_{10} . It can be seen that an excellent agreement exists between experimental results and model predictions. Notice that for an initial styrene mole fraction of $f_{10} = 0.6$ an azeotropic copolymerization system is obtained. In Figure 3, model predictions and experimental measurements on number- and weight-average molecular weights are shown for an initial styrene mole fraction of 0.8. The model predicts successfully the variation of M_n and M_w with conversion. It should be noted that the observed large increase in the values of both M_n and M_w at high conversions is an additional evidence that terminal double bond reaction and gel effect are significant for this system. Figures 4 and 5 illustrate the variation of the termination rate constants k_{t11} and k_{t22} vs the overall monomer conversion for the five different values of f_{10} . It is apparent that both termination rate constants exhibit a significant decrease with conversion similar to the one found in homopolymerizations.¹² It is also clear that the initial mole fraction of styrene greatly affects the diffusion-controlled termination rate constant. The contribution of the residual termination rate constant to k_{tji} (see eq 27), depicted by the plateau in the variation of k_{t11} and k_{t22} with respect to the overall conversion after the appearance of the gel effect (see Figures 4 and 5), depends on the residual concentration of the respective monomers. Finally, in Figures 6 and 7 the diffusion-controlled propagation rate constant, k_{p11} , and the initiator efficiency are plotted against conver-

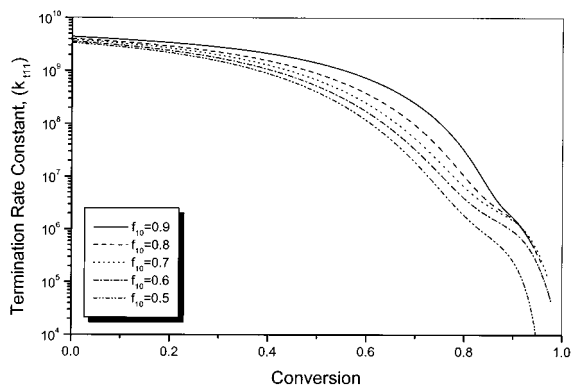


Figure 4. Variation of the termination rate constant k_{t11} with respect to the overall monomer conversion (conditions same as Figure 1).

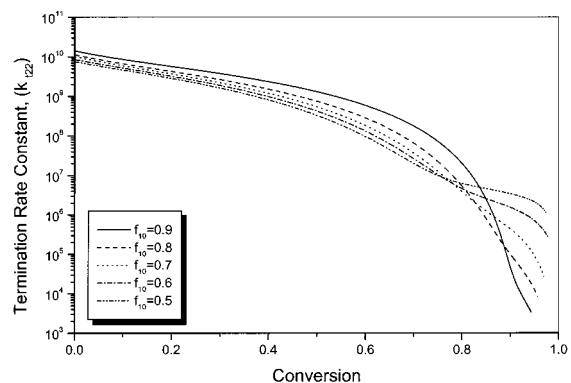


Figure 5. Variation of the termination rate constant k_{t22} with respect to the overall monomer conversion (conditions same as Figure 1).

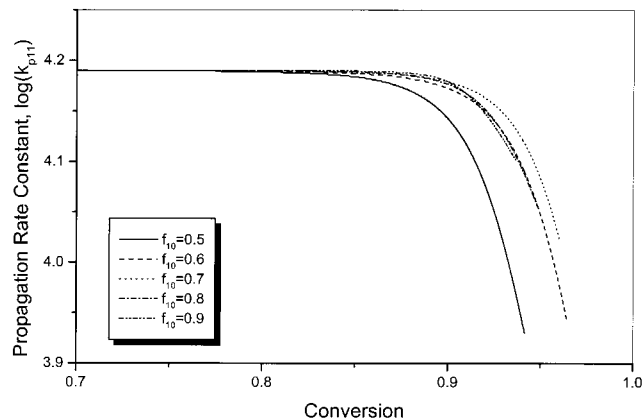


Figure 6. Variation of the propagation rate constant k_{p11} with respect to the overall monomer conversion (conditions same as Figure 1).

sion. It can be seen that the corresponding values of conversion at which these two quantities become diffusion-controlled depend on the initial styrene mole fraction and, hence, the composition of the reaction mixture. Notice that the initiator efficiency exhibits a dramatic decrease (e.g., by almost 3 orders of magnitude) due to the extremely limited mobility of the primary radicals at very high conversions. Although the diffusion model developed in this work describes satisfactorily the copolymerization of SAN, our knowledge of the kinetic or/and diffusion model parameters may be imperfect. This gives rise to the important problem of parameter sensitivity. In the present study, a sensitivity analysis was carried out to analyze the effect of the overlap

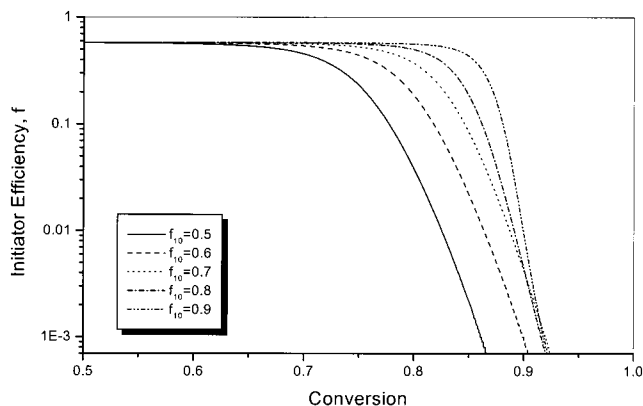


Figure 7. Variation of the initiator efficiency with respect to the overall monomer conversion (conditions same as Figure 1).

factor, γ_p (e.g., a critical parameter appearing in the diffusion model), on the final values of M_n , M_w , and polymerization time for a given value of the overall monomer conversion. As expected, the sensitivity of the model output variables with respect to the variation in γ_p exhibited a maximum value in the gel effect region. On the other hand, at low and high monomer conversions the output variables were less sensitive to variations in γ_p . Specifically, it was found that a 15% variation in the value of γ_p (e.g., from 0.17 to 0.20) resulted in a 4.5% increase in the final value of M_w , a 5.1% increase in the value of M_w , and in a 7.6% decrease of the polymerization time from their corresponding nominal values.

Bulk Copolymerization of Styrene–Methyl Methacrylate. The bulk copolymerization of styrene–methyl methacrylate (STMMA) was assumed to proceed in single phase. Model predictions were compared with the experimental data of O’Driscoll and Huang⁴¹ on monomer conversion, copolymer composition, and average molecular weights for three different initial monomer compositions. The copolymerizations were carried at 60 °C in the presence of 2,2’-azodiisobutyrate (AIBME) initiator.

The self-termination of “live” polymer chains, ending in an MMA monomer unit, was assumed to occur mainly by disproportionation, while the termination of “live” polymer chains, ending in a styrene unit, was assumed to occur exclusively by combination.^{12,40} The cross-termination rate constants were estimated in terms of the respective homopolymer termination rate constants (see eq 34). Chain transfer reactions to monomer, polymer, and initiator molecules were assumed to be negligible.²² The numerical values of all kinetic rate constants for the styrene–methyl methacrylate copolymerization system are reported in Table 3. In Table 4 the values of the physical and transport properties of the system are presented.

In Figure 8, conversion–time histories are shown for three values of the initial styrene mole fraction, f_{10} . Continuous and broken lines represent model predictions while discrete points denote experimental conversion measurements. Apparently, a very good agreement exists between model predictions and experimental measurements. It can be seen that the reaction rate decreases as the initial styrene mole fraction increases, due to the lower value of the styrene propagation rate constant. In Figure 9, the cumulative copolymer composition is plotted with respect to the overall monomer

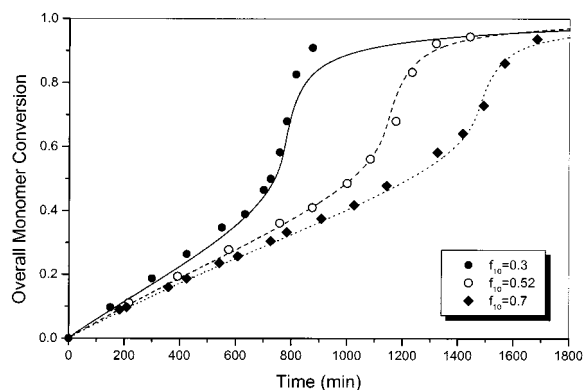


Figure 8. Predicted and experimental conversion–time histories for styrene–methyl methacrylate copolymerization (polymerization temperature 60 °C, $[I_0] = 0.01$ M AIBME, experimental data from ref 41).

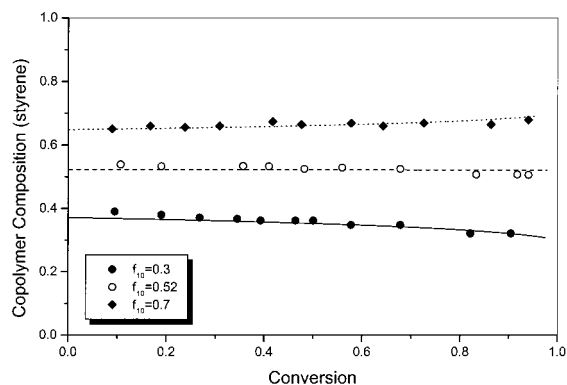


Figure 9. Cumulative copolymer composition of styrene with respect to the overall monomer conversion (conditions same as in Figure 8).

Table 3. Kinetic Rate Constants for the STMA Copolymerization

$k_{p11} = 6.54 \times 10^8 \exp(-7051/RT)$ (L/mol min) (ref 12)
$k_{p22} = 2.95 \times 10^7 \exp(-4353/RT)$ (L/mol min) (ref 12)
$r_1 = 0.52$; $r_2 = 0.46$ (ref 30)
$k_{tc11} = 7.53 \times 10^{10} \exp(-1677/RT)$ (L/mol min) (ref 43)
$k_{td22} = 5.88 \times 10^9 \exp(-701/RT)$ (L/mol min) (ref 12)
$k_{td11} = 0$; $k_{tc22} = 0$; $\varphi_t = 25$
$k_d = 60 \times \exp(33.1 - 14800/T)$ (1/min) (ref 12)

conversion for three different values of f_{10} . It is evident that a very good agreement exists between experimental results and model predictions. Notice that, for an initial styrene mole fraction of $f_{10} = 0.52$, an azeotropic copolymerization is obtained. In Figure 10, model predictions and experimental measurements on number- and weight-average molecular weights are plotted for an initial styrene mole fraction of 0.3. An excellent agreement exists between model predictions and experimental measurements on both M_n and M_w . Figures 11 and 12 illustrate the variation of the two termination rate constants k_{t11} and k_{t22} with respect to the overall monomer conversion for three different values of f_{10} . It is apparent that both termination rate constants are greatly affected by the monomer composition of the reaction mixture. Moreover, they both exhibit a similar behavior with that observed in the SAN system. Finally, the effect of monomer conversion and initial styrene mole fraction on the respective propagation rate constants (k_{p11} and k_{p22}) is depicted in Figures 13 and 14.

Bulk Copolymerization of *p*-Methylstyrene–Methyl Methacrylate. The bulk copolymerization of *p*-methylstyrene–methyl methacrylate system (*p*-MST-

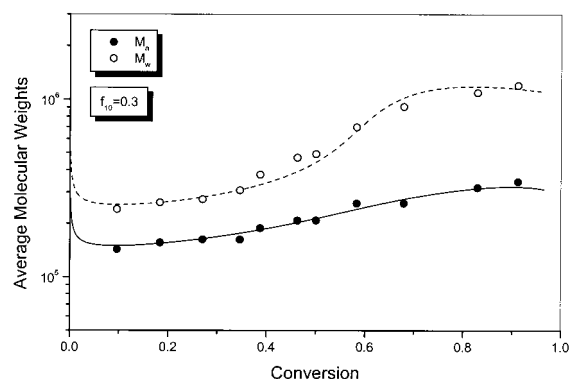


Figure 10. Weight- and number-average molecular weights with respect to the overall monomer conversion (conditions same as Figure 8).

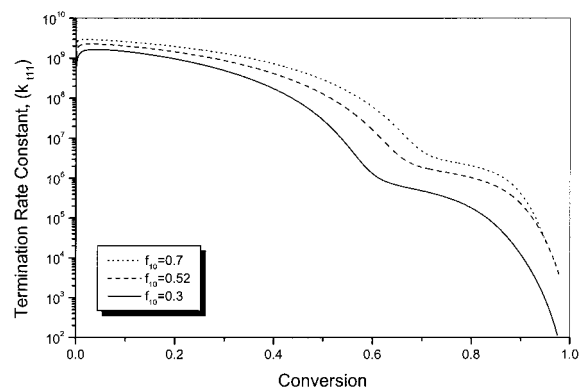


Figure 11. Variation of the termination rate constant k_{t11} with respect to the overall monomer conversion (conditions same as Figure 8).

Table 4. Physical and Transport Properties for the STMA Copolymerization System

$d_{m1} = 0.9236 - 0.887 \times 10^{-3}(T - 273.15)$ (g/cm ³) (ref 12)
$d_{m2} = 0.968 - 1.225 \times 10^{-3}(T - 273.15)$ (g/cm ³) (ref 12)
$d_{p1} = 1.085 - 0.887 \times 10^{-3}(T - 273.15)$ (g/cm ³) (ref 45)
$d_{p2} = 1.212 - 8.45 \times 10^{-4}(T - 273.15)$ (g/cm ³) (ref 40)
$MW_1 = 104.14$; $MW_2 = 100.13$; $M_{f1} = 101.12$; $f_0 = 0.4$ (ref 12)
$\delta_1 = 7.4$ Å; $\delta_2 = 6.9$ Å (ref 12)
$X_{c01} = 385$; $X_{c02} = 100$ (ref 12)
$\epsilon_{110}/D_{10} = 31.04$; $\epsilon_{120}/D_{10} = 49.75$ (s/cm ²) (ref 12)
$\alpha_p = F_{n1}\alpha_{p1} + (1 - F_{n1})\alpha_{p2}$
$\alpha_{p1} = 4.5 \times 10^{-4}$; $\alpha_{p2} = 3.0 \times 10^{-4}$; $\alpha_{m1} = 6.2 \times 10^{-4}$;
$\alpha_{m2} = 2.9 \times 10^{-4}$ (K ⁻¹) (ref 6)
$\alpha_{p0} = 0.025$; $\alpha_{m10} = 0.040$; $\alpha_{m20} = 0.011$ (ref 6)
$T_{gm1} = 185.0$ K (ref 1); $T_{gm2} = 159.15$ K (ref 18)
$V_{m1}^* = 0.912$; $V_{m2}^* = 0.868$; $V_{p1}^* = 0.835$; $V_{p2}^* = 0.788$;
$V_1^* = 0.846$; (cm ³ /g) (calcd)
$r_{e1} = 16.9$; $r_{e2} = 17.0$ Å; $r_e = F_{n1}r_{e1} + (1 - F_{n1})r_{e2}$ (Kuhn's
segment length) (ref 47)
$\gamma_m = 0.30$; $\gamma_1 = 0.30$; $\gamma_p = 0.18$; $\alpha_{seg} = 0.2$
$D_{m10} = 1.97 \times 10^{-8}$ (cm ² /s) (ref 12); $D_{m20} = 8.27 \times 10^{-10}$ (cm ² /s)
$\log(\eta_1) = 528.64 \times (1/T - 1/276.71)$ cP
$\log(\eta_2) = 453.25 \times (1/T - 1/254.92)$ cP; $G_{12} = -0.309$
$[\eta]_{0.7} = 7.16 \times 10^{-5} M_w^{0.51}$; $[\eta]_{0.52} = 7.0 \times 10^{-5} M_w^{0.51}$;
$[\eta]_{0.3} = 9.73 \times 10^{-5} M_w^{0.47}$ (1/g) (ref 46)

MMA) was considered to proceed in one phase. Model predictions were compared with the experimental measurements of Jones et al.¹⁸ on monomer conversion and residual monomer mole fraction obtained for three different initial monomer compositions. The copolymerizations were carried out at 60 °C in the presence of 2,2'-azobis(isobutyronitrile) (AIBN) initiator.

The self-termination of “live” polymer chains ending in a *p*-methylstyrene monomer unit was assumed to occur by combination, while the self-termination of “live”

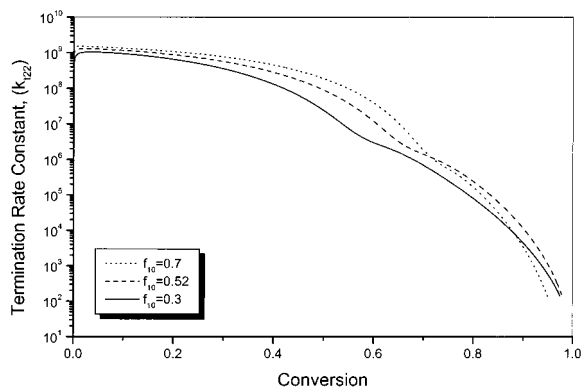


Figure 12. Variation of the termination rate constant k_{t22} with respect to the overall monomer conversion (conditions same as Figure 8).

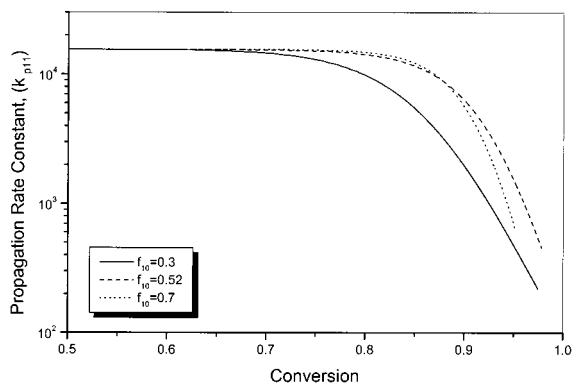


Figure 13. Variation of the propagation rate constant k_{p11} with respect to the overall monomer conversion (conditions same as Figure 8).

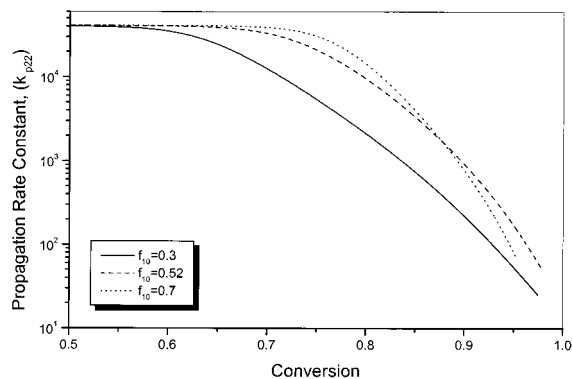


Figure 14. Variation of the propagation rate constant k_{p22} with respect to the overall monomer conversion (conditions same as Figure 8).

Table 5. Kinetic Rate Constants for the *p*-MSt–MMA Copolymerization

$k_{p11} = 6.306 \times 10^8 \exp(-7068/RT)$ (L/mol min) (ref 42)
$k_{p22} = 2.95 \times 10^7 \exp(-4353/RT)$ (L/mol min) (ref 12)
$r_1 = 0.419$; $r_2 = 0.498$ (ref 18)
$k_{tc11} = 1.41 \times 10^{11} \exp(-1976/RT)$ (L/mol min) (ref 42)
$k_{td22} = 5.88 \times 10^9 \exp(-701/RT)$ (L/mol min) (ref 12)
$k_{td11} = 0$; $k_{tc22} = 0$; $\varphi_t = 10$
$k_d = 6.32 \times 10^{16} \exp(-30660/RT)$ (1/min) (ref 12)

polymer chains ending in an MMA monomer unit was assumed to occur by disproportionation.^{12,42} The respective cross-termination rate constants were estimated by eq 34. Chain transfer reactions to monomer, polymer, and initiator were neglected.¹⁸ In Table 5 the numerical values of the kinetic rate constants employed in the simulation of the *p*-methylstyrene–methyl methacrylate

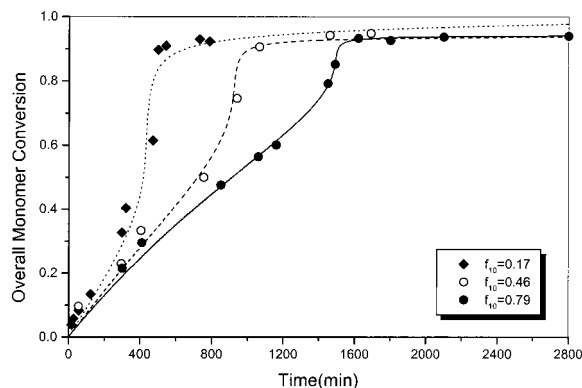


Figure 15. Predicted and experimental conversion–time histories for *p*-methylstyrene–methyl methacrylate copolymerization (polymerization temperature 60 °C, $[I_0] = 0.0157$ M AIBN, experimental data from ref 18).

Table 6. Physical and Transport Properties for the *p*-MSt–MMA Copolymerization System

$d_{m1} = 0.9261 - 9.18 \times 10^{-4}(T - 273.15)$
$d_{m2} = 0.968 - 1.225 \times 10^{-3}(T - 273.15)$ (g/cm ³) (ref 12)
$d_p = 1.11$ (g/cm ³) (ref 18)
$MW_1 = 118.17$; $MW_2 = 100.13$; $M_f = 68.1$; $f_0 = 0.58$ (ref 12)
$\delta_1 = 7.4$ Å; $\delta_2 = 6.9$ Å (ref 12)
$X_{c01} = 385$; $X_{c02} = 100$ (ref 12)
$\epsilon_{110}/D_{10} = 50.0$; $\epsilon_{120}/D_{10} = 372.38$ (s/cm ²) (ref 12)
$\alpha_p = F_{n1}\alpha_{p1} + (1 - F_{n1})\alpha_{p2}$
$\alpha_{p1} = 4.8 \times 10^{-4}$; $\alpha_{p2} = 3.0 \times 10^{-4}$; $\alpha_{m1} = 1.0 \times 10^{-4}$;
$\alpha_{m2} = 2.9 \times 10^{-4}$ (K ⁻¹) (ref 40)
$\alpha_{p0} = 0.025$; $\alpha_{m10} = 0.025$; $\alpha_{m20} = 0.011$ (ref 6)
$T_{gm1} = 150.15$ K (ref 1); $T_{gm2} = 159.15$ K; $T_{gp} = 387.15$ (ref 18)
$V_1^* = 0.926$; $V_{m2}^* = 0.868$; $V_{p1}^* = 0.859$; $V_{p2}^* = 0.788$;
$V_1^* = 0.912$ (cm ³ /g) (calcd)
$r_{e1} = 17.7$; $r_{e2} = 17.0$ Å; $r_c = F_{n1}r_{e1} + (1 - F_{n1})r_{e2}$ (Kuhn's
segment length) (ref 47)
$\gamma_m = 0.25$; $\gamma_1 = 0.25$; $\gamma_p = 0.18$; $\alpha_{seg} = 0.20$
$D_{m10} = 1.97 \times 10^{-8}$ (cm ² /s) (ref 9); $D_{m20} = 8.27 \times 10^{-10}$ (cm ² /s)
$\log(\eta_1) = 528.64 \times (1/T - 1/276.71)$ cP (ref 12)
$\log(\eta_2) = 453.25 \times (1/T - 1/254.92)$ cP (ref 12); $G_{12} = -0.409$
$[\eta]_{0.79} = 7.16 \times 10^{-5} M_w^{0.51}$; $[\eta]_{0.46} = 7.0 \times 10^{-5} M_w^{0.51}$;
$[\eta]_{0.17} = 9.73 \times 10^{-5} M_w^{0.47}$ (l/g) (ref 46)

copolymerization system are reported. In Table 6 the physical and transport properties of the system are presented.

In Figure 15 conversion–time histories are plotted for three different values of the initial *p*-methylstyrene mole fraction, f_{10} . Continuous and broken lines represent model predictions while discrete points denote the experimental conversion measurements. A very good agreement between model predictions and experimental measurements is obtained. It is also evident that as the initial mole fraction of *p*-methylstyrene decreases the polymerization rate increases due to the higher value of the propagation rate constant of methyl methacrylate. It should be pointed out that in all cases examined the final value of the overall monomer conversion was less than 100% due to the appearance of the glass effect. In Figure 16 the residual mole fraction of *p*-methylstyrene is plotted with respect to the overall monomer conversion. It can be seen that an excellent agreement exists between experimental results and model predictions. Finally, the effect of monomer conversion and initial *p*-methylstyrene mole fraction on the termination rate constants (k_{t11} and k_{t22}) is depicted in Figures 17 and 18.

Conclusions

Based on the original developments of Achilias and Kiparissides¹² and the generalized free-volume theory

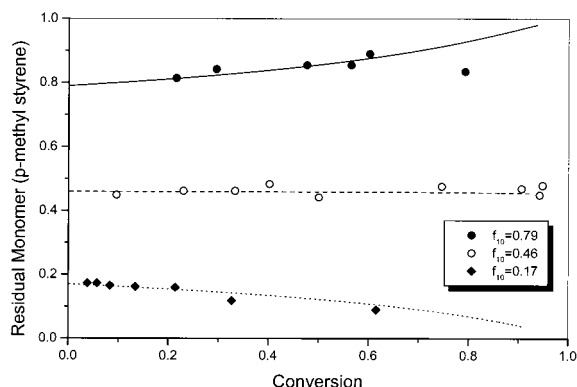


Figure 16. Residual mole fraction of *p*-methylstyrene with respect to the overall monomer conversion (conditions same as in Figure 15).

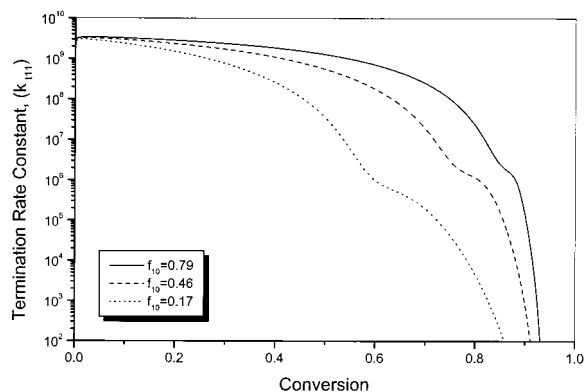


Figure 17. Variation of the termination rate constant k_{t11} with respect to the overall monomer conversion (conditions same as Figure 15).

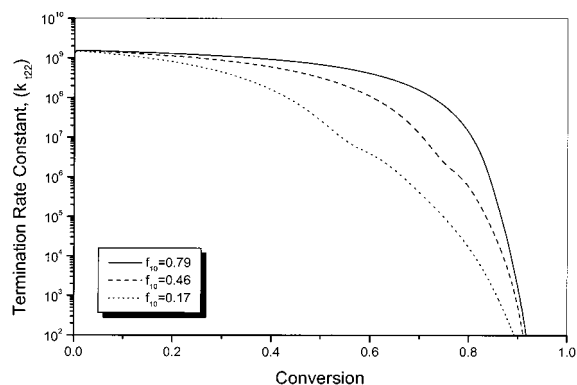


Figure 18. Variation of the termination rate constant k_{t22} with respect to the overall monomer conversion (conditions same as Figure 15).

of Vrentas and Duda for ternary systems,²³ a comprehensive mathematical framework was developed to describe diffusion-controlled phenomena in free-radical copolymerization systems. The effects of overall monomer conversion and residual monomer concentrations on the termination and propagation rate constants as well as on the initiator efficiency were quantified using a parallel model description, comprising a reaction-limited term and a diffusion-controlled contribution. The predictive capabilities of the proposed model were demonstrated by the successful simulation of experimental data on conversion, copolymer composition, and molecular weight averages reported for three copolymerization systems (i.e., styrene–acrylonitrile, styrene–methyl methacrylate, and *p*-methylstyrene–methyl meth-

acrylate). Present efforts are focused on the extension of the model to multicomponent free-radical polymerizations.

Nomenclature

- A_p = proportionality rate constant (cm^3/mol)
- AIBME = 2,2'-azodiisobutyrate
- AIBN = 2,2'-azobis(isobutyronitrile)
- D = diffusion coefficient (cm^2/s)
- d = density (g/cm^3)
- $D_{n,m}$ = concentration of dead polymer with $n + m$ monomer units
- f = initiator efficiency
- f_D = diffusion-controlled term of the initiator efficiency
- F_{seg} = factor representing the probability of two radicals two react when their active centers come into close proximity
- F_n, F_w = cumulative number- and weight-average copolymer composition
- G_{12} = binary interaction parameter for the calculation of the viscosity of a mixture
- I = initiator concentration (mol/L)
- j_c = entanglement spacing
- k_B = Boltzmann constant ($1.3806 \times 10^{-23} \text{ J}/\text{K}$)
- k_d = initiator decomposition rate constant ($\text{L}/\text{mol}/\text{min}$)
- k_{dp} = terminal double bond reaction rate constant ($\text{L}/\text{mol}/\text{min}$)
- k_t = chain transfer to monomer/chain transfer agent rate constant ($\text{L}/\text{mol}/\text{min}$)
- k_{tp} = chain transfer to polymer rate constant ($\text{L}/\text{mol}/\text{min}$)
- k_i = initiation reaction rate constant ($\text{L}/\text{mol}/\text{min}$)
- k_p = propagation rate constant ($\text{L}/\text{mol}/\text{min}$)
- k_t = overall rate constant for termination reaction ($\text{L}/\text{mol}/\text{min}$)
- k_{tc} = termination by combination rate constant ($\text{L}/\text{mol}/\text{min}$)
- k_{td} = termination by disproportionation rate constant ($\text{L}/\text{mol}/\text{min}$)
- k_t^d = diffusion-controlled termination rate constant ($\text{L}/\text{mol}/\text{min}$)
- k_t^{res} = residual termination rate constant ($\text{L}/\text{mol}/\text{min}$)
- M = monomer concentration (mol/cm^3)
- MW = molecular weight
- M_n, M_w = number- and weight-average molecular weight (g/mol)
- N_A = Avogadro's number ($6.023 \times 10^{23} \text{ molecules}/\text{mol}$)
- R^* = primary radical
- $R_{n,m}$ = concentration of "live" radical with $n + m$ monomer units
- R = universal gas constant ($1.9872 \text{ cal}/\text{mol}/\text{K}$)
- R_T = the average number of both monomer sequences occurring in a copolymer per 100 monomer units
- r_B = distance of the chain end from the sphere center (\AA)
- r_M = production rate of monomer ($\text{mol}/\text{cm}^3/\text{min}$)
- r_t, r_m = effective reaction radius (cm)
- r_e = Kuhn's segment length (\AA)
- r_1, r_2 = reactivity ratios
- r_{11}, r_{12} = radius of initiator reaction sphere and diffusion sphere, respectively (cm)
- R_H = hydrodynamic radius (cm)
- S = solvent concentration (mol/cm^3)
- T = temperature (K)
- T_g = glass transition temperature (K)
- \bar{T}_{gp} = mean glass transition temperature of the homopolymers (K)
- V = reactor volume (cm^3)
- V_{FH} = average free volume of the mixture (cm^3/g)
- V^* = critical hole free volume (cm^3/g)
- V_{pj} = molar volume of the copolymer jumping unit (cm^3/g)
- x_i = mole fraction of monomer i
- X = conversion
- X_{c0} = critical degree of polymerization for entanglements

Greek Letters

α = difference in thermal expansion coefficients above and below T_g (1/K)

α_{i0} = fractional free volume at the glass transition temperature of component i

α_{seg} = parameter for the calculation of segmental diffusion

γ = overlap factor

δ = average root-mean-square end-to-end distance per square root of the number of the monomer units in a chain (Å)

ϵ_1 = proportionality constant ($=k_{t0}/k_{p0}$)

η = viscosity (cP)

$[\eta]$ = intrinsic viscosity of the polymer (cm³/g)

λ = moments of the live radical distribution

μ = moments of the dead polymer distribution

ξ = ratio of the critical molar volume of the jumping unit the critical molar volume of the polymer jumping unit

τ = parameter for the calculation of the termination radius

φ = volume fraction

φ_t = cross termination rate parameter

ω = weight fraction

Subscripts

I = initiator

m = monomer

p = polymer

s = solvent

t = termination

0 = initial conditions

1, 2 = monomer 1, 2

Superscripts

* = critical

1, 2 = monomer 1, 2 as a terminal unit of a growing chain

References and Notes

- Zhu, S.; Tian, Y.; Hamielec, A. E.; Eaton, D. R. *Polymer* **1990**, *31*, 154.
- Sack, R.; Schulz, G. V.; Meyerhoff, G. *Macromolecules* **1988**, *21*, 3345.
- Cardenas, J. N.; O'Driscoll, K. F. *J. Polym. Sci., Polym. Chem. Ed.* **1976**, *14*, 883.
- Marten, F. L.; Hamielec, A. E. *ACS Symp. Ser.* **1979**, No. 104, 43.
- Tullig, T. J.; Tirrell, M. *Macromolecules* **1981**, *14*, 1501.
- Soh, S. K.; Sundberg, D. C. *J. Polym. Sci., Polym. Chem. Ed.* **1982**, *20*, 1331.
- Chiu, W. Y.; Carratt, M. G.; Soong, S. D. *Macromolecules* **1983**, *16*, 348.
- Stickler, M. *Makromol. Chem.* **1983**, *184*, 2563.
- Mita, I.; Horie, K. *J. Macromol. Sci., Rev. Macromol. Chem. Phys.* **1987**, *C27*, 91.
- Achilias, D. S.; Kiparissides, C. *J. Appl. Polym. Sci.* **1988**, *35*, 1303.
- Buback, M. *Makromol. Chem.* **1990**, *191*, 1575.
- Achilias, D. S.; Kiparissides, C. *Macromolecules* **1992**, *25*, 3739.
- Panke, D. *Macromol. Theory Simul.* **1995**, *4*, 759.
- Ray, A. B.; Saraf, D. N.; Gupta, S. K. *Polym. Eng. Sci.* **1995**, *35*, 1290.
- Hoppe, S.; Renken, A. *Polym. React. Eng.* **1998**, *6*, 1.
- Cavin, L.; Rouge, A.; Meyer, Th.; Renken, A. *Polymer* **2000**, *41*, 3925.
- Garcia-Rubio, L. H.; Lord, M. G.; MacGregor, J. F.; Hamielec, A. E. *Polymer* **1985**, *26*, 2001.
- Jones, K. M.; Bhattacharya, D.; Brash, J. L.; Hamielec, A. E. *Polymer* **1986**, *27*, 602.
- Bhattacharya, D.; Hamielec, A. E. *Polymer* **1986**, *27*, 611.
- Yaraskavitch, I. M.; Brash, J. L.; Hamielec, A. E. *Polymer* **1987**, *28*, 489.
- Hwang, W.-H.; Yoo, K.-Y.; Rhee, H.-K. *J. Appl. Polym. Sci.* **1997**, *64*, 1015.
- Sharma, D. K.; Soane, D. S. (Soong) *Macromolecules* **1988**, *21*, 700.
- Neogi, P. *Diffusion in Polymers*; Marcel Dekker: New York, 1996; p 165.
- Vrentas, J. S.; Duda, J. L.; Ling, H. C. *J. Polym. Sci., Polym. Phys. Ed.* **1984**, *22*, 459.
- Vrentas, J. S.; Duda, J. L.; Ling, H. C. *J. Appl. Polym. Sci.* **1985**, *30*, 4499.
- Vrentas, J. S.; Duda, J. L. *J. Polym. Sci., Polym. Phys. Ed.* **1977**, *15*, 403.
- Vrentas, J. S.; Duda, J. L. *J. Polym. Sci., Polym. Phys. Ed.* **1977**, *15*, 417.
- Haward, R. N. *J. Macromol. Sci., Rev. Macromol. Chem.* **1970**, *C4*, 191.
- Hong, S. U. *J. Appl. Polym. Sci.* **1996**, *61*, 833.
- Suzuki, H.; Mathot, V. B. F. *Macromolecules* **1989**, *22*, 1380.
- Reid, R. C.; Prausnitz, J. M.; Poling, B. E. *The Properties of Gases & Liquids*, 4th ed.; McGraw-Hill: New York, 1988; p 474.
- Crowley, T. J.; Choi, K. Y. *J. Comput. Chem. Eng.* **1999**, *23*, 1153.
- North, A. M. *Macromol. Chem.* **1965**, *83*, 15.
- Litvinenko, G. I.; Kaminsky, V. A. *Prog. React. Kinet.* **1994**, *19*, 139.
- Buback, M.; Huckestein, B.; Russel, G. T. *Makromol. Chem. Phys.* **1994**, *195*, 539.
- Achilias, D. S.; Kiparissides, C. *Polymer* **1994**, *35*, 1714.
- Baltsas, A.; Achilias, D. S.; Kiparissides, C. *Macromol. Theory Simul.* **1996**, *5*, 477.
- Achilias, D. S.; Kiparissides, C. *J. Macromol. Sci., Rev. Macromol. Chem. Phys.* **1992**, *C32*, 183.
- Garcia-Rubio, L. H. An Experimental Investigation On The Free Radical Synthesis And Characterization Of Styrene-Acrylonitrile Copolymers. Ph.D. Thesis, McMaster University, 1981.
- Tefera, N.; Weickert, G.; Westerterp, K. R. *J. Appl. Polym. Sci.* **1997**, *63*, 1663.
- O'Driscoll, K. F.; Huang, J. *Eur. Polym. J.* **1989**, *25*, 629.
- Baltsas, A.; Achilias, D. S.; Kiparissides, C. *Polymer* **1992**, *33*, 5018.
- Pittman-Bejger, T. P. Real-Time Control and Optimization of Batch Free-Radical Copolymerization Reactors. Ph.D. Thesis, University of Minnesota, 1982.
- Balaraman, K. S.; Nadkarni, V. M.; Mashelkar, R. A. *Chem. Eng. Sci.* **1986**, *41*, 1357.
- Crowley, T. J.; Choi, K. Y. *J. Appl. Polym. Sci.* **1998**, *70*, 1017.
- Bradrup, J., Immergut, E., Eds.; *Polymer Handbook*; Wiley-Interscience: New York, 1989.
- Aharoni, S. M. *Macromolecules* **1986**, *19*, 426.

MA010999Q